Interplay of frustration and magnetic field in the two-dimensional quantum antiferromagnet $Cu(tn)Cl_2$

A. Orendáčová,* E. Čižmár, L. Sedláková, J. Hanko, M. Kajňaková, M. Orendáč, and A. Feher
Center of Low Temperature Physics, Faculty of Science, P. J. Šafárik University, Park Angelinum 9, 041 54 Košice, Slovakia

J. S. Xia, L. Yin, D. M. Pajerowski, and M. W. Meisel
Department of Physics and the National High Magnetic Field Laboratory, University of Florida, Gainesville, Florida 32611-8440, USA

V. Zeleňák
Institute of Chemistry, Faculty of Sciences, P. J. Šafárik University, Moyzesova 16, 041 54 Košice, Slovakia

S. Zvyagin and J. Wosnitza
Hochfeld-Magnetlabor Dresden (HLD), Forschungszentrum Dresden-Rossendorf, D-01314 Dresden, Germany
(Received 17 June 2009; revised manuscript received 31 August 2009; published 21 October 2009)

Specific heat and ac magnetic susceptibility measurements, spanning low temperatures ($T \geq 40$ mK) and high-magnetic fields ($B \leq 14$ T), have been performed on a two-dimensional (2D) antiferromagnet $Cu(tn)Cl_2$ (tn=1,3-diaminopropane=$C_3H_{10}N_2$). The compound represents a $S=1/2$ spatially anisotropic triangular antiferromagnet realized by a square lattice with nearest-neighbor ($J/k_B=3$ K), frustrating next-nearest-neighbor ($0<J'/J<0.6$), and interlayer ($|J''/J| \approx 10^{-3}$) interactions. The absence of long-range magnetic order down to $T=60$ mK in $B=0$ and the T^2 behavior of the specific heat for $T \leq 0.4$ K and $B \geq 0$ are considered evidence of a high degree of 2D magnetic order. In fields lower than the saturation field, $B_{sat}=6.6$ T, a specific heat anomaly, appearing near 0.8 K, is ascribed to bound vortex-antivortex pairs stabilized by the applied magnetic field. The resulting magnetic phase diagram is remarkably consistent with the one predicted for a square lattice without a frustrating interaction, expect that B_{sat} is shifted to values lower than expected. Potential explanations for this observation, as well as the possibility of a Berezinski-Kosterlitz-Thouless (BKT) phase transition in a spatially anisotropic triangular magnet with the collinear Néel ground state, are discussed.

DOI: 10.1103/PhysRevB.80.144418 PACS number(s): 75.40.−s, 75.10.Jm

I. INTRODUCTION

Two-dimensional (2D) quantum antiferromagnets have attracted a significant amount of theoretical and experimental attention due to the unconventional magnetic properties resulting from the interplay between quantum fluctuations and geometrical frustration.[1–3] One example is the $S=1/2$ spatially anisotropic triangular antiferromagnet, which can be treated as a square lattice with the nearest-neighbor (nn) interaction J and frustrating next-nearest-neighbor (nnn) interaction J', Fig. 1. The nnn coupling plays an important role in the determination of the ground state properties of the 2D antiferromagnet. For example, a relatively weak nnn coupling does not suppress collinear Néel order characteristic for the ideal square lattice ($J'=0$), and the Néel phase persists up to $J' \approx 0.6J$. For stronger frustration, the system enters a dimerized phase, and for $J' > 0.9J$, a three sublattice spiral Néel order is stabilized. Further strengthening of J' leads to the gradual melting of the spiral order and the establishment of a disordered spin liquid state, which is smoothly transformed into a one-dimensional (1D) decoupled spin chain in the $J' \to \infty$ limit.[4–8] The presence of an applied magnetic field provides an additional constraint. Considerable theoretical interest in the spin liquid phase ($J'/J > 1$) in a magnetic field[9–11] was triggered by experimental studies of Cs_2CuCl_4, a spatially anisotropic triangular antiferromagnet with $J'/J \approx 3$.[12–14]

Recently, $Cu(tn)Cl_2$ (tn=1,3-diaminopropane=$C_3H_{10}N_2$) has been identified as a potential model system for the realization of the spatially anisotropic triangular Heisenberg antiferromagnet from the collinear Néel phase.[15] For $Cu(tn)Cl_2$ studied in $B=0$, no evidence for long-range magnetic order was observed down to 60 mK, and the data suggested antiferromagnetic intralayer interaction strengths of $J/k_B=3$ K and $0<J'/J<0.6$, while the interlayer coupling is $|J''/J| \approx 10^{-3}$. These interactions refer to the $S=1/2$ Heisenberg Hamiltonian

$$\mathcal{H} = J\sum_{nn} \mathbf{S}_i \cdot \mathbf{S}_j + J'\sum_{nnn} \mathbf{S}_i \cdot \mathbf{S}_j + J''\sum_{i,k} \mathbf{S}_i \cdot \mathbf{S}_k, \qquad (1)$$

where i,j label intralayer spins and k labels the interlayer ones.

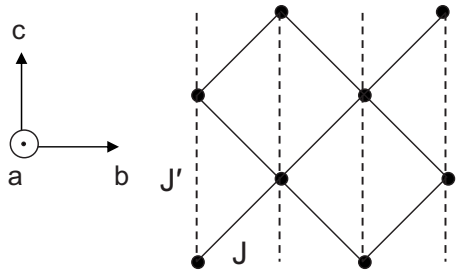

FIG. 1. Realization of Heisenberg model of a spatially anisotropic triangular lattice within a single *bc* layer in $Cu(tn)Cl_2$. The layers are stacked along the *a* direction. The full circles denote Cu^{2+} ions.

The motivation of the present work was to explore the response of $Cu(tn)Cl_2$ in $B \neq 0$, especially at low temperatures, $T \ll J/k_B$. For this purpose, experimental specific heat and ac susceptibility studies were performed over a wide range of temperatures (40 mK $\leq T \leq$ 10 K) and magnetic fields ($0 \leq B \leq 14$ T). The low value of the intralayer exchange coupling affords easy access to the magnetic phases below and above the saturation field. On the basis of the magnetic field induced features observed in the specific heat and ac susceptibility, a magnetic phase diagram is constructed and analyzed within a model of a field induced Berezinski-Kosterlitz-Thouless (BKT) phase transition recently theoretically predicted for the $S=1/2$ Heisenberg antiferromagnet on a pure 2D square lattice with zero nnn coupling.[16] It is noteworthy that the long-range orderings in some quasi-2D, square lattice systems, namely, $Sr_2CuO_2Cl_2$ and several $Cu(pyz)_2$-based materials (pyz=pyrazine), have been placed close to the BKT transition.[17–19]

It is important to note that for $B=0$, the BKT transition is expected at finite temperatures for only 2D planar magnets.[20,21] However, the application of the magnetic field to a 2D Heisenberg antiferromagnet, which is the case for $Cu(tn)Cl_2$, introduces competition between the magnetic field and the exchange interaction. In the classical limit, the magnetic field forces the spins to lie nearly in the plane perpendicular to the field, but some canting can remain in this state called the spin-flop phase.[22,23] In other words, the magnetic field acts as an effective easy-plane anisotropy, and field-induced BKT behavior is only expected for 2D antiferromagnets, since for isotropic 2D ferromagnets, the application of the magnetic field leads to full polarization of the moments along the field direction.

Our presentation begins with a discussion of the sample and experimental details, which are followed by a description of our experimental results. Next, an analysis and a discussion of the results are given before the salient points are assembled into the magnetic phase diagram. The paper concludes with a summary and some comments about possible future directions.

II. SAMPLE AND EXPERIMENTAL DETAILS

The crystal structure of $Cu(tn)Cl_2$ (tn =1,3-diaminopropane=$C_3H_{10}N_2$), established at 150 K, is orthorhombic (space group $Pna2_1$) with the lattice parameters $a=17.956$ Å, $b=6.859$ Å, and $c=5.710$ Å.[15] The structure consists of covalently bonded ladders running along the c-axis, while the adjacent ladders in the bc-plane are linked through intermolecular N-H$\cdots$Cl hydrogen bonds formed by all four H atoms of the amino groups. In the a direction, the layers are connected by weak C-H$\cdots$Cl type interactions. The strongly elongated octahedra coordinating the Cu(II) ions stabilize the d_{z^2} electronic ground state. Consequently, the propagation of exchange pathways between Cu(II) ions leads to the formation of a spatially anisotropic triangular lattice in the bc-plane (Fig. 1). Typically, the Cu(II) ion can be described as a Heisenberg spin with a weak g-factor anisotropy, and this situation applies to $Cu(tn)Cl_2$ since $g_{\parallel}/g_{\perp} < 1.1$.[15] Such a small g-factor anisotropy commonly leads to very weak exchange anisotropy, and as a consequence, the isotropic Heisenberg model can be employed to analyze data obtained on randomly oriented powders.

The synthesis of all $Cu(tn)Cl_2$ samples followed the established procedure,[15] which produces polycrystals that are powdered and pressed into pellets (nominally 3 mg to 10 mg) for the specific heat studies or placed into appropriate specimen holders for the magnetic susceptibility investigations. A sample with a mass of 26 mg was used in the ac magnetic measurements.

Using several experimental probes and instruments, the specific heat measurements were performed over the temperature range from 100 mK to 10 K and in magnetic fields up to 14 T. More specifically, the studies in the millikelvin temperature region and in magnetic fields up to 2.5 T were performed using a relaxation calorimeter[24] mounted on a dilution refrigerator. A commercial (Quantum Design PPMS) device was used for the specific heat studies over the temperature range from 1.8 to 10 K and in fields up to 9 T, while the low temperature studies down to 0.35 K and in fields up to 14 T utilized another commercial instrument equipped with a ^{3}He insert. In each instance, the contribution of the background addenda was determined in separate runs. Finally, the separate study of the specific heat of a diamagnetic isomorph, $Zn(tn)Cl_2$, allowed the phonon contribution to be determined.

The magnetic susceptibility studies were performed with ac (232 Hz) mutual inductance coils mounted on a dilution refrigerator equipped with a 10 T magnet. With the sample immersed in pure ^{3}He that provided intimate thermal contact with the mixing chamber, the in-phase and out-of-phase signals of the susceptibility were recorded by a two channel lock-in amplifier. Typically the data were obtained by isothermal field sweeps at a rate of 50 mT/min, and the data were independent of the direction of the field sweep. The position of the zero response of the susceptibility in high fields was established by assuming the saturation magnetization was achieved at the lowest temperatures and in the highest fields. This assumption is consistent with the analysis of the high-field specific heat results, as will be explained in subsequent sections, and allows an obvious background contribution to be subtracted. The field dependence of the low field ($B < 1$ T) response is surprisingly temperature independent, except for a constant shift, and this part of the signal is conjectured to be associated with a background effect. Nevertheless, since the low-field region cannot presently be unambiguously modeled, it is presented in the susceptibility data plots and kept as a part of the integration yielding the M/M_{sat} versus B at 40 mK.

III. EXPERIMENTAL RESULTS

A. Specific heat in $B \neq 0$

Evidence of the presence of 2D magnetic correlations was initially observed as a round maximum in the temperature dependence of the total specific heat, $C_{TOT}(T)$, near 2 K in $B=0$,[15] and our present work found this feature to evolve with magnetic fields up to 9 T, Fig. 2. In fact, the influence of

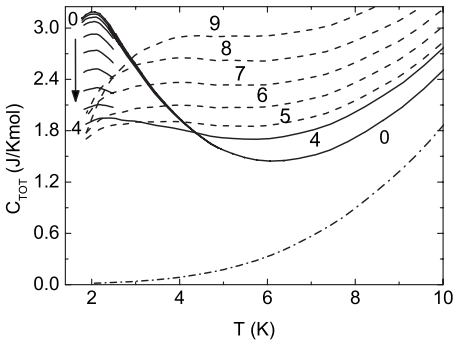

FIG. 2. Temperature dependence of the total specific heat, C_{TOT}, of $Cu(tn)Cl_2$ in various magnetic fields. Solid lines represent data for $B=0$, 0.5, 0.75, 1, 1.5, 2, 2.5, 3, 3.5, and 4 T, while the dashed lines correspond to $B=5$, 6, 7, 8, and 9 T. The dot-dashed line represents the specific heat of the diamagnetic isomorph $Zn(tn)Cl_2$.

the magnetic field can be separated into two regimes. For $B<4$ T, the height of the specific heat maximum, C_{max}, decreases with increasing field while its temperature, T_{max}, remains nearly unchanged, whereas for $B>4$ T, C_{max} increases with increasing field and T_{max} shifts toward higher temperatures. The phonon contribution to the specific heat can be approximated by the specific heat of the diamagnetic isomorph $Zn(tn)Cl_2$, Fig. 2. These high-temperature measurements were extended to lower temperatures in $B \leq 2.5$ T, and the results of the total specific heat are shown in Fig. 3. These studies revealed the presence of an anomaly appearing at about 0.8 K when $B \neq 0$, and this feature develops with increasing magnetic field (inset of Fig. 3). The magnetic field and temperature dependences of this anomaly were measured in $B \leq 14$ T, Fig. 4, where this feature reaches a maximum in 4 T at 0.8 K and decreases in magnitude, with a simultaneous shift to lower temperatures, until its presence is no longer resolved in fields greater than 7 T.

B. Magnetic susceptibility in $B \leq 10$ T

The results of isothermal ac susceptibility studies in $B \leq 10$ T are shown in Fig. 5, and no significant hysteresis was observed between the up and down sweeps. The data do

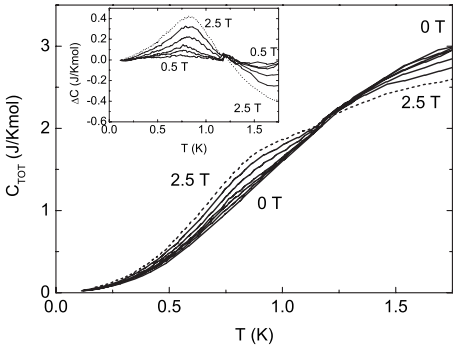

FIG. 3. Temperature dependence of the total specific heat of $Cu(tn)Cl_2$ in $B=0$, 0.5, 0.75, 1, 1.5, 2, and 2.5 T. Inset: Temperature dependence of the difference $\Delta C=[C(T,B)-C(T,0)]$ between the total specific heat in finite and zero magnetic fields.

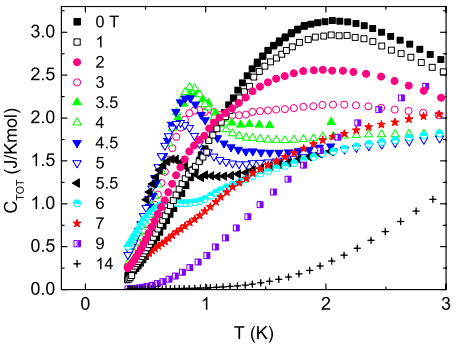

FIG. 4. (Color online) Temperature dependence of the total specific heat of $Cu(tn)Cl_2$ in various magnetic fields.

not possess any sharp anomalies corresponding to a phase transition, but the appearance of a shoulder near 6 T corresponds to the field where the low-temperature specific heat anomaly vanishes. Unlike the low-temperature specific heat anomaly, the shoulder survives up to 1 K, suggesting that it is associated with the saturation magnetic field B_{sat}.

IV. ANALYSIS AND DISCUSSION

A. Magnetic correlations in $B=0$

As stated earlier, previous specific heat studies in $B=0$ did not indicate any magnetic phase transition down to 60 mK, and a clear quadratic dependence was observed at low temperatures. The latter coincides with the expected 2D character of short-range magnetic correlations,[15] since the spin wave analysis of low-dimensional models with nn interactions predicts a T^2 behavior for the low-temperature specific heat of square and triangular lattices and a T dependence for a linear-chain model.[25] The absence of a λ-like anomaly associated with magnetic ordering is another intriguing feature of the specific heat data.

In the absence of the frustration ($J'=0$), the ordering temperature T_N of the isotropic square lattice with interlayer coupling J'' can be expressed as[26,27]

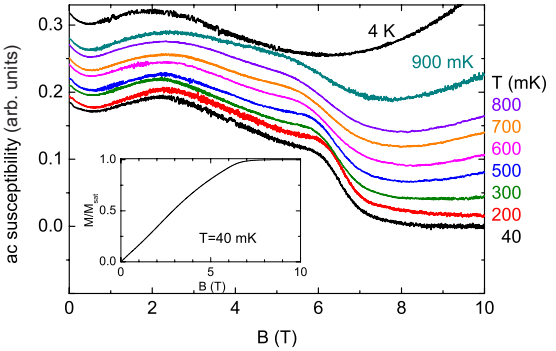

FIG. 5. (Color online) Magnetic field dependence of isothermal ac susceptibility of $Cu(tn)Cl_2$ at various temperatures. Inset: Magnetic field dependence of the normalized isothermal magnetization at 40 mK.

$$k_B T_N = J'' \left(\frac{M}{M_0}\right)^2 \left(\frac{\xi}{a}\right)^2, \tag{2}$$

where M/M_0 is a staggered magnetization, a represents a lattice constant, and ξ is an intralayer correlation length given by

$$\frac{\xi}{a} = 0.5 \frac{\exp\left(\frac{2\pi\rho_s}{k_B T}\right)}{1 + \left(\frac{k_B T}{2\pi\rho_s}\right)}. \tag{3}$$

Here, ρ_s is a spin stiffness, and for the isotropic square lattice with intralayer nn exchange coupling J, it can be expressed as $\rho_s \cong 0.18J$. Using the parameters $|J''/k_B| \approx 3$ mK, $|J/k_B| \approx 3$ K, determined in Ref. 15, and $(M/M_0)^2 \approx 0.3$, a phase transition in $Cu(tn)Cl_2$ might be expected at $T_N \approx 0.8$ K. The absence of the phase transition down to 60 mK may suggest a significant reduction of both the spin stiffness and the staggered magnetization as a consequence of frustrating nnn J' coupling.[4–6,26,27] Apart from the aforementioned reduction of staggered magnetization, the weakness of the interlayer coupling can also lead to the absence of a detectable phase transition at finite temperatures in specific heat measurements. Recent Monte Carlo studies of the specific heat of an isotropic square lattice with various interlayer couplings revealed that, for $J''/J \lesssim 0.015$, the peak associated with the phase transition vanishes.[28] Since $|J''/J| \approx 10^{-3}$ for $Cu(tn)Cl_2$, the ordering effects might not be observed in the specific heat even in the absence of frustration. While experimental studies of $Cu(pyz)_2(ClO_4)_2$ are consistent with this scenario,[29] the observation of a phase transition in the specific heat of $Cu(H_2O)_2(C_2H_8N_2)SO_4$ with a comparable J''/J ratio shows the need to consider additional effects.[30]

B. Magnetic correlations in $B \neq 0$

1. Specific heat for $T \geq J/k_B$

After the subtraction of the phonon contribution, approximated by the specific heat of the diamagnetic isomorph $Zn(tn)Cl_2$ (Fig. 2), two different regimes can be distinguished in the behavior of C_{max} for $T > 1.8$ K. For $B \lesssim 4$ T, C_{max} decreases with increasing field while T_{max} remains nearly unchanged, whereas for $B \gtrsim 5$ T, C_{max} increases with increasing field and T_{max} shifts toward higher temperatures, Fig. 6. Such a qualitative behavior has been predicted for a linear (1D) chain with *nn* coupling $\mathcal{J}$,[31,32] where the crossover between the two regimes occurs at a saturation field

$$g\mu_B B_{sat} = 2\mathcal{J}. \tag{4}$$

Using $g = 2.12$ and $\mathcal{J}/k_B = 4$ K, which correspond to the best estimates of the parameters resulting from the linear chain model as applied to $Cu(tn)Cl_2$ in Ref. 15, Eq. (4) predicts $B_{sat} = 5.6$ T, a value that coincides rather well with the crossover region appearing between 4 and 6 T. However, in comparison with the linear chain, which is characterized by a decrease in T_{max} with increasing field for fields lower than B_{sat} and an increase for higher fields, the observed shift of T_{max} with respect to the magnetic field behaves differently.

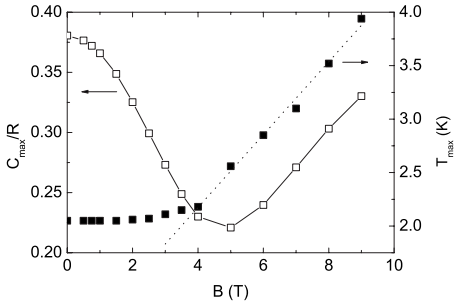

FIG. 6. Magnetic field dependence of the value for the maximum of the $Cu(tn)Cl_2$ magnetic specific heat, C_{max}, divided by the gas constant R (open squares). The solid line is a guide for eyes. Magnetic field dependence of the temperature, T_{max}, denoting the position of C_{max} (full squares). The broken line is a linear fit (see text).

Alternatively, the effect of an external magnetic field on the short-range correlations and the thermodynamic properties of a square lattice have been theoretically investigated,[16] and the saturation field is

$$g\mu_B B_{sat} = 4J. \tag{5}$$

For $Cu(tn)Cl_2$, this model predicts $B_{sat} = 8.4$ T, which is too high to correspond to the observed crossover region.

This qualitative comparison of the limiting 1D and 2D theoretical models with the experimental data suggests the existence of two phases in $Cu(tn)Cl_2$, namely, a low-field phase stable in the magnetic fields below the crossover region where antiferromagnetic correlations prevail and a high-field paramagnetic phase stabilized in the fields above the crossover region. However, the atypical magnetic field dependence of T_{max} suggests a more complex low-field phase. Indeed, a closer look at the behavior shown in the Fig. 6 reveals that, within experimental uncertainty, T_{max} remains constant for $B < 2$ T, before increasing slightly in the fields from 2 T to 4 T, and then experiencing a quasilinear increase for the fields above 4 T, as demonstrated by a linear fit performed in the range from 4 to 9 T.

2. Specific heat for $T \leq J/k_B$

The quantitative analysis of magnetic specific heat, C_M, at temperatures $T < 0.4$ K and $B < 2.5$ T reveals the T^2 dependence, as can be seen in Fig. 7, where the data are plotted as $C_M T^2$ vs T^4. This approach assumes the magnetic specific heat can be expressed as a sum of a/T^2 and bT^2 terms, where the first term corresponds to the contribution of the nuclear spins and/or three-dimensional (3D) long-range correlations between electronic spins, and the second term is associated with 2D short-range correlations. A set of linear fits of the individual $C_M T^2$ vs T^4 dependences for fixed magnetic field was performed in the temperature range from nominally 150 to 400 mK. The fitting procedure revealed a very small value of the coefficient a, which varied from $(1.5 \pm 0.5) \times 10^{-4}$ JK/mol for $B = 0$ to $(2.0 \pm 0.5) \times 10^{-4}$ JK/mol for $B = 2.5$ T, and these results are similar to the ones reported for other Cu(II) materials.[13] Contrastingly, a significant, monotonic rise of the coefficient b [in units of J/(K^3 mol)]

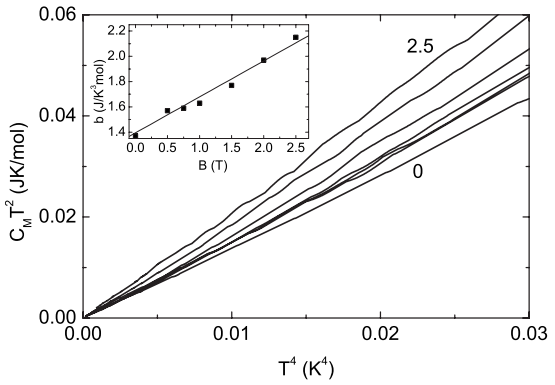

FIG. 7. $C_M T^2$ vs T^4 dependence for $Cu(tn)Cl_2$ in $B=0$, 0.5, 0.75, 1, 1.5, 2, and 2.5 T. Inset: Magnetic field dependence of the coefficient b, Eq. (6). The solid line represents a linear fit.

with increasing magnetic field was detected, and this behavior is described by

$$b(B) = 1.36 + 0.30B, \tag{6}$$

as shown in the inset of Fig. 7. The observed low temperature T^2 behavior of $C_M(T)$ suggests the preservation of the mainly 2D character of the magnetic correlations in $B \neq 0$. Furthermore, the field does not introduce an energy gap to the excitation spectrum, which remains gapless as expected for the square lattice in magnetic fields below the saturation value.[16]

To more precisely trace the position of the low-temperature peak, T_p, appearing at about 0.8 K, as a function of magnetic field, the specific heat in zero magnetic field was chosen as a reference background that was subtracted from the specific heat in nonzero magnetic field, inset of Fig. 8. Using the low-field data obtained in the same way (inset of Fig. 3), the magnetic field dependence of T_p can be extracted (Fig. 8). It can be seen that a naive extrapolation to zero field provides $T_p \approx 0.7$ K, which is close to the value of the transition temperature $T_N \approx 0.8$ K estimated for the isotropic square lattice. Additional experimental work is needed to either verify the suggestion that the weakness of the interlayer coupling prevents the observation of the phase transition in the $B=0$ specific heat study or to establish that the two temperatures are just coincidently close.

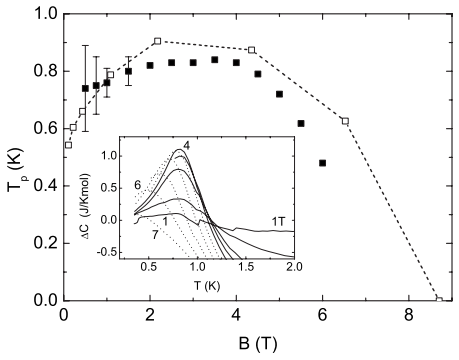

FIG. 8. Magnetic field dependence of the peak position, T_p, of the low temperature specific heat anomalies (full squares) in $Cu(tn)Cl_2$. The theoretical prediction for the field induced BKT phase transition for the isotropic square lattice is denoted by the open squares and the broken line. Inset: Temperature dependence of the difference between the specific heat in finite and zero magnetic field. The solid lines represent $B=1$, 2, 3, 3.5, and 4 T, and the dashed lines correspond to $B=4.5$, 5, 5.5, 6, and 7 T.

An extrapolation of the high-field experimental data yields $B(T_p \to 0) \approx 6-7$ T, which is lower than $B_{sat}=8.4$ T calculated for the isotropic square lattice. Finally, to determine B_{sat} from the specific heat data, we analyzed the $C_M(T)$ data in 9 and 14 T. While the peak height of $C_M(T)$ in 9 T is still much lower than $C_{max}/R=0.438$, the theoretical prediction for the $S=1/2$ ideal paramagnet (Fig. 6), the corresponding $B=14$ T value of $C_{max}/R=0.42$ is close to the expected result. For $B > B_{sat}$, a gap Δ opens in the spin excitation spectrum, developing linearly with magnetic field as[13]

$$\Delta = g\mu_B(B - B_{sat}). \tag{7}$$

In the temperature region where thermal fluctuations overcome the interlayer coupling and $T < \Delta/k_B$, a 2D character of magnon spectra can be expected, resulting in[13]

$$C_M(T) \approx \frac{1}{T}\exp(-\Delta/k_B T). \tag{8}$$

Fitting the $C_M(T<1$ K, $B=9$ T) and $C_M(T<3$ K, $B=14$ T) data yields $\Delta/k_B=3.4$ K and 10.5 K, respectively, and it follows from Eq. (7) that $B_{sat}=6.6 \pm 0.1$ T, when assuming $g=2.12$. It is important to note that the significant differences between the observed $B_{sat}=6.6$ T and the 8.4 T value expected for the isotropic square lattice indicate that $Cu(tn)Cl_2$ is indeed affected by the presence of frustrating nnn interactions, since the interlayer coupling is expected to increase B_{sat} as[19]

$$g\mu_B B_{sat} = 4J + 2J''. \tag{9}$$

3. AC susceptibility for $T \leq J/k_B$

The ac susceptibility data, $\chi(T,B) = \partial M/\partial B$, can be integrated to obtain the magnetization $M(T,B)$, as shown in the inset of Fig. 5, and $M(T \to 0, B)$ data are commonly used to establish B_{sat}, if the saturation plateau is accessible. However, in many instances, the transition to the fully polarized state is broadened by several effects, including issues related to finite temperature, orientation of the microcrystals, and finite size effects, so an extrapolation is used to establish a value for B_{sat}. Our ac susceptibility data shown in Fig. 5 suggest $B_{sat}=6.5 \pm 0.2$ T for $T \leq 200$ mK (when considering B_{sat} as the midpoint of the region where $\chi(B)$ is most strongly changing), and this value agrees with the one extracted from the analysis of the C_M data at 9 and 14 T.

The crossover region, ΔB_{sat}, that spans from the region from about 6 to 7 T at low temperature, Fig. 5, merits further analysis. For example, when $k_B T \approx 0.1J$, thermal smearing of the crossover is not expected. Alternatively, the powder character of the sample might induce a scatter of B_{sat} that can be evaluated as $B_{sat}^{\parallel} - B_{sat}^{\perp}$. Previous electron paramagnetic resonance studies provided values for the anisotropic g-tensor of $g_{\parallel}=2.25$ and $g_{\perp}=2.05$.[15] Assuming an ideal square lattice and taking $J/k_B=3$ K, then

$$B_{\mathrm{sat}}^{\parallel,\perp} = \frac{4J}{g_{\parallel,\perp}\mu_B}, \tag{10}$$

yields $|\Delta B_{\mathrm{sat}}| \leq 0.8$ T, which is less than but similar in magnitude to the observed width of the crossover.

C. Magnetic phase diagram of $Cu(tn)Cl_2$

Prior to building the magnetic phase diagram, the correlations between the shift of T_p and the position of high-temperature specific heat maximum T_{max} with respect to the magnetic field are worth noting (Figs. 6 and 8). The monotonic increase of T_p with increasing magnetic field up to about 2 T corresponds to the relative field independence of T_{max} in this field region. The relative field independence of T_p in the field from 2 to 4 T corresponds to the slight increase of T_{max}, and finally, the rather rapid decrease of T_p above 4 T corresponds to a linear increase of T_{max}.

This relationship between the low-temperature anomaly and the high-temperature maximum suggests that the magnetic field mainly affects the short-range correlations. This interpretation is supported by the monotonic increase of T_p observed in low fields, and this behavior is typical for the BKT transition theoretically predicted in the classical limit for two-dimensional antiferromagnets in uniform magnetic fields.[33,34] Quantum Monte Carlo studies of the $S=1/2$ isotropic square lattice in a magnetic field also revealed field-induced XY behavior, and a BKT transition at a finite temperature, T_{BKT}, was identified in the wide range of magnetic fields.[16] Since a sufficiently small nnn coupling J' does not change the character of the ground state of a 2D antiferromagnet on the square lattice, the response of such system should be essentially the same as a nonfrustrated system with $J'=0$. Consequently, the measured T_p vs B dependence has been compared to the theoretical prediction of T_{BKT} vs B calculated for $g=2.12$ and $J/k_B=3$ K, and the comparison yields good agreement between the theoretical results and the data (Fig. 8). It should be noted that the authors of Ref. 16 identified the BKT phase transitions at T_{BKT}, which lies below T_p. However, the determination of T_{BKT} directly from the experiment is not as straightforward as the determination of T_p. From this point of view, one must be aware that the experimental determinations of T_{BKT} are overestimated.

Recent quantum Monte Carlo calculations of a B vs T magnetic phase diagram performed for the system of a tetragonal lattice with intralayer coupling J and interlayer coupling J'' revealed that, for sufficiently large spatial anisotropy J/J'', the system preserves nonmonotonic B vs T behavior typical for the BKT transition on the ideal square lattice.[19] The enhancement of the critical temperatures and the saturation field with respect to the ideal 2D case is another effect of the interlayer coupling. The predictions were compared with the experimentally established phase diagram of $[Cu(HF_2)(pyz)_2]BF_4$, a representative of the quasi-2D Heisenberg square lattice with a finite temperature phase transition to 3D long-range order in zero magnetic field, and excellent agreement was found.[19] Unlike the phase diagram of $Cu(tn)Cl_2$, the experimental data of $[Cu(HF_2)(pyz)_2]BF_4$ are significantly shifted above the theoretical prediction for the ideal square lattice model. The fact that our data lie significantly lower, i.e., below the theoretical predictions for the BKT transition (Fig. 8), supports the conjecture about the important presence of frustration.

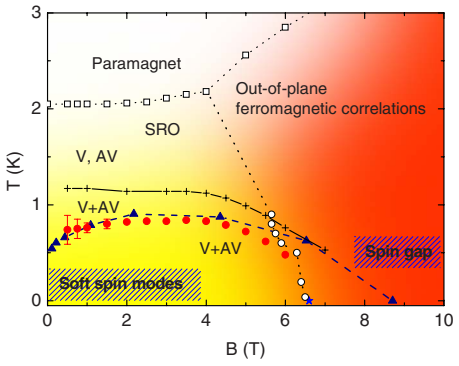

FIG. 9. (Color online) Extended magnetic phase diagram of $Cu(tn)Cl_2$. The open squares represent the T_{max} vs B dependence, while the pluses (+) correspond to the line constructed from the condition that $\delta_T S(T,B) - \delta_T S(T,0) = 0$, see text. The theoretically predicted BKT transition and the experimental T_p vs B dependence are denoted by full triangles and full circles, respectively. Open circles correspond to the positions of the midpoints in the shoulders of ac susceptibility data. The star represents the B_{sat} as extracted from an analysis of the specific heat data measured in 9 T and 14 T. The dotted and solid lines are guides for eyes. The regions of short-range order (SRO) and free or bound vortex (V) and antivortex (AV) pairs are identified. Detailed descriptions of each $B-T$ region are given in the text.

Considering all the ac susceptibility and specific heat features together, we can identify the major regions in the extended magnetic phase diagram for $Cu(tn)Cl_2$ as a triangular magnet from the collinear Néel phase (Fig. 9). At temperatures above 2 K, the system behaves as a paramagnet in all magnetic fields. The paramagnetic region is separated by the line determined by the T_{max} vs B dependence. At temperatures below the line, 2D antiferromagnetic correlations develop, forming free vortices (V) and antivortices (AV) in the xy plane. The vortices are stabilized by the magnetic field, whose direction defines the z-axis in the spin space. The formation of bound V-AV pairs begins at temperatures below a line derived from the requirement that the difference of the entropy derivatives $[\delta_T S(T,B) - \delta_T S(T,0)]$ is zero.[16] This quantity equals the difference of the specific heat $[C(T,B) - C(T,0)]$ divided by temperature T. The intensity of the pairing process culminates at the temperatures defined by the position of the low-temperature specific heat anomaly. As was shown in the theoretical studies of the BKT transition,[16,19] the temperature of the BKT transition itself is about 20%–30% lower than the position of the specific heat maximum. Consequently for $Cu(tn)Cl_2$, the potential BKT transition can be expected at temperatures lower than the critical line constructed from the T_p vs B data.

Above the critical magnetic field region determined from the position of the high-field shoulder in the isothermal ac susceptibility data, out-of-plane ferromagnetic correlations induced by the magnetic field are stabilized, while in-plane spin correlations show paramagnetic behavior.[35] In this re-

gion, a spin gap appears in the excitation spectrum, and this gap was detected by the exponential character of the low temperature specific heat measured in 9 T. As shown in the phase diagram, the induced ferromagnetic correlations survive up to the temperatures on the critical line T_{max} vs B. In accordance with the theoretical predictions for the square lattice,[35] the formation of the out-of-plane ferromagnetic correlations begins at higher temperatures in fields above 4 T, as indicated by the linear dependence of T_{max} vs. B above 4 T.

The onset of quasi-long-range order (QLRO), induced by the field due to the stabilization of bound V-AV pairs expected for the unfrustrated square lattice at sufficiently low temperatures, should be reflected by the smaller entropy increase in finite magnetic field than in zero field.[16] In other words, the presence of the V-AV pairs should lead to negative values of $[C(T,B)-C(T,0)]$ at low temperatures. However, as can be seen from the insets of Figs. 3 and 8, in $Cu(tn)Cl_2$, the difference remains positive down to the lowest temperatures. The increasing specific heat with magnetic field can be ascribed to the combined effect of the interlayer coupling and the existence of soft spin modes, likely associated with the frustrated nnn coupling, which can prevent the system from achieving full QLRO.

V. SUMMARY

The response of $Cu(tn)Cl_2$ to an externally applied magnetic field has been investigated by specific heat and ac susceptibility studies at low temperatures, $T \geq 40$ mK, and in magnetic fields up to 14 T. Specific features induced by the magnetic field in the behavior of both quantities allowed a magnetic phase diagram, whose regions are rooted in the presence of a high degree of short-range order, to be constructed. The quadratic temperature dependence of the specific heat observed below 0.4 K and in magnetic fields up to, at least, 2.5 T arises from the predominantly 2D character of magnetic correlations and identifies a gapless excitation spectrum as predicted for the isotropic square lattice. Furthermore, in finite magnetic fields up to 6 T, a field induced anomaly appears near 0.8 K, and this feature is associated with the existence of a BKT transition theoretically predicted for the isotropic square lattice.[16] This association merits microscopic studies and will be the focus of future neutron and/or muon scattering studies. The absence of a phase transition in zero magnetic field is interpreted as a consequence of a combined effect of the weak interlayer coupling and the frustration within the magnetic layers. The saturation magnetic field value, as extracted from the specific heat and ac susceptibility data, deviates significantly from the one predicted for an isotropic square lattice, and this result is conjectured to be a consequence of the frustrating magnetic interactions, in the *bc* layer, that have been confirmed recently by quantum mechanical calculations.[36]

Finally, it is noteworthy that a T^2 dependence of the specific heat has been reported for several frustrated 2D systems in zero magnetic field and was ascribed to various scenarios. While only a weak field dependence of the low-temperature specific heat has been observed in Kagomé[37] and triangular[38] compounds, the linear increase of the b coefficient, as observed in $Cu(tn)Cl_2$, points to the fact that even an infinitesimal field is able to introduce the changes. This sensitivity also supports the applicability of the BKT model to $Cu(tn)Cl_2$; however, only to some extent. In the spin wave region, the magnetic field should decrease the specific heat and, correspondingly, the b coefficient, as expected for the square lattice. Since the opposite tendency was observed, our experimental data suggest the presence of soft spin modes that are possibly connected with frustration and interlayer coupling. A spin wave analysis of the triangular magnet from the Néel phase in a magnetic field would be desirable to elucidate these observed differences. Recently, the BKT description has been successfully used[39] to explain the 2D spin freezing transition observed in $NiGa_2S_4$, a model system for the $S=1$ isotropic triangular Heisenberg lattice.[40]

In conclusion, the analysis of experimental data suggests that the $S=1/2$ spatially anisotropic triangular magnet from the collinear Néel phase undergoes a BKT transition induced by an applied magnetic field. Theoretical studies of the collinear Néel phase in a magnetic field are necessary to specify the proper range of J, J' parameters where the BKT transition can occur. Microscopic magnetic studies of $Cu(tn)Cl_2$, possibly employing neutron and/or muon scattering techniques, are needed to clarify the nature of the ground state in zero and nonzero magnetic fields.

ACKNOWLEDGMENTS

One of us (A.O.), has benefited from many fruitful discussions with Tommasso Roscilde and Eva Pavarini. We are grateful Sasha Chernyshev for the discussions about low temperature specific heat in a magnetic field. This work was supported, in part, by VEGA under Grant No. 1/0078/09, Project No. APVV-0006-07, ESF RNP program "Highly Frustrated Magnetism," NSF under Grant No. DMR-0701400, the NHMFL via cooperative agreement NSF under Grant No. DMR-0654118 and the State of Florida, Deutsche Physikalische Gesellschaft (DPG), and EuroMagNET II. Material support from U.S. Steel Košice s.r.o. is greatly acknowledged.

*alzbeta.orendacova@upjs.sk

[1] M. Kohno, O. A. Starykh, and L. Balents, Nat. Phys. **3**, 790 (2007).
[2] S. Sachdev, Nat. Phys. **4**, 173 (2008).
[3] C. Xu and S. Sachdev, Phys. Rev. B **79**, 064405 (2009).
[4] J. Merino, R. H. McKenzie, J. B. Marston, and C. H. Chung, J. Phys.: Condens. Matter **11**, 2965 (1999).
[5] Z. Weihong, R. H. McKenzie, and R. R. P. Singh, Phys. Rev. B **59**, 14367 (1999).
[6] L. O. Manuel and H. A. Ceccatto, Phys. Rev. B **60**, 9489 (1999).

[7] M. Q. Weng, D. N. Sheng, Z. Y. Weng, and R. J. Bursill, Phys. Rev. B **74**, 012407 (2006).
[8] T. Pardini and R. R. P. Singh, Phys. Rev. B **77**, 214433 (2008).
[9] M. Y. Veillette and J. T. Chalker, Phys. Rev. B **74**, 052402 (2006).
[10] J. Alicea and M. P. A. Fisher, Phys. Rev. B **75**, 144411 (2007).
[11] O. A. Starykh and L. Balents, Phys. Rev. Lett. **98**, 077205 (2007).
[12] R. Coldea, D. A. Tennant, A. M. Tsvelik, and Z. Tylczynski, Phys. Rev. Lett. **86**, 1335 (2001).
[13] T. Radu, H. Wilhelm, V. Yushankhai, D. Kovrizhin, R. Coldea, Z. Tylczynski, T. Lühmann, and F. Steglich, Phys. Rev. Lett. **95**, 127202 (2005).
[14] Y. Tokiwa, T. Radu, R. Coldea, H. Wilhelm, Z. Tylczynski, and F. Steglich, Phys. Rev. B **73**, 134414 (2006).
[15] V. Zeleňák, A. Orendáčová, I. Císařová, J. Černák, O. V. Kravchyna, J.-H. Park, M. Orendáč, A. G. Anders, A. Feher, and M. W. Meisel, Inorg. Chem. **45**, 1774 (2006).
[16] A. Cuccoli, T. Roscilde, R. Vaia, and P. Verrucchi, Phys. Rev. B **68**, 060402(R) (2003).
[17] P. A. Goddard, J. Singleton, P. Sengupta, R. D. McDonald, T. Lancaster, S. J. Blundell, F. L. Pratt, S. Cox, N. Harrison, J. L. Manson, H. I. Southerland, and J. A. Schlueter, New J. Phys. **10**, 083025 (2008).
[18] F. Xiao, F. M. Woodward, C. P. Landee, M. M. Turnbull, C. Mielke, N. Harrison, T. Lancaster, S. J. Blundell, P. J. Baker, P. Babkevich, and F. L. Pratt, Phys. Rev. B **79**, 134412 (2009).
[19] P. Sengupta, C. D. Batista, R. D. McDonald, S. Cox, J. Singleton, L. Huang, T. P. Papageorgiou, O. Ignatchik, T. Herrmannsdörfer, J. L. Manson, J. A. Schlueter, K. A. Funk, and J. Wosnitza, Phys. Rev. B **79**, 060409(R) (2009).
[20] J. M. Kosterlitz and D. J. Thouless, J. Phys. C **5**, L124 (1972); **6**, 1181 (1973).
[21] V. L. Berezinskii, Zh. Eksp. Teor. Fiz. **59**, 907 (1970).
[22] M. Holtschneider, W. Selke, and R. Leidl, Phys. Rev. B **72**, 064443 (2005).
[23] A. Cuccoli, G. Gori, R. Vaia, and P. Verrucchi, J. Appl. Phys. **99**, 08H503 (2006).
[24] S. Riegel and G. Weber, J. Phys. E **19**, 790 (1986).
[25] B. Bernu and G. Misguich, Phys. Rev. B **63**, 134409 (2001).
[26] S. Chakravarty, B. I. Halperin, and D. R. Nelson, Phys. Rev. Lett. **60**, 1057 (1988).
[27] A. V. Chubukov, S. Sachdev, and J. Ye, Phys. Rev. B **49**, 11919 (1994).
[28] P. Sengupta, A. W. Sandvik, and R. R. P. Singh, Phys. Rev. B **68**, 094423 (2003).
[29] T. Lancaster, S. J. Blundell, M. L. Brooks, P. J. Baker, F. L. Pratt, J. L. Manson, M. M. Conner, F. Xiao, C. P. Landee, F. A. Chaves, S. Soriano, M. A. Novak, T. P. Papageorgiou, A. D. Bianchi, T. Herrmannsdörfer, J. Wosnitza, and J. A. Schlueter, Phys. Rev. B **75**, 094421 (2007).
[30] M. Kajňaková, M. Orendáč, A. Orendáčová, A. Vlček, J. Černák, O. V. Kravchyna, A. G. Anders, M. Bałanda, J.-H. Park, A. Feher, and M. W. Meisel, Phys. Rev. B **71**, 014435 (2005).
[31] J. C. Bonner and M. E. Fischer, Phys. Rev. **135**, A640 (1964).
[32] A. Klümper, Eur. Phys. J. B **5**, 677 (1998).
[33] D. P. Landau and K. Binder, Phys. Rev. B **24**, 1391 (1981).
[34] A. S. T. Pires, Phys. Rev. B **50**, 9592 (1994).
[35] T. Roscilde, Ph.D. thesis, University of Pavia, 2002.
[36] E. Pavarini (private communication).
[37] A. P. Ramirez, B. Hessen, and M. Winklemann, Phys. Rev. Lett. **84**, 2957 (2000).
[38] S. Nakatsuji, Y. Nambu, H. Tonomura, O. Sakai, S. Jonas, C. Broholm, H. Tsunetsugu, Y. Qiu, and Y. Maeno, Science **309**, 1697 (2005).
[39] C.-H. Chern, Phys. Rev. B **78**, 020403(R) (2008).
[40] D. E. MacLaughlin, Y. Nambu, S. Nakatsuji, R. H. Heffner, Lei Shu, O. O. Bernal, and K. Ishida, Phys. Rev. B **78**, 220403(R) (2008).